Dalton Transactions

RSC Publishing

PAPER

A theoretical study of the mechanisms of oxidation of ethylene by manganese oxo complexes†

Cite this: *Dalton Trans.*, 2013, **42**, 14411

Albert Aniagyei, Richard Tia* and Evans Adei

The mechanisms of oxidation of ethylene by manganese–oxo complexes of the type MnO_3L (L = O^-, Cl, CH_3, OCH_3, Cp, NPH_3) have been explored on the singlet, doublet, triplet and quartet potential energy surfaces at the B3LYP/LACVP* level of theory and the results discussed and compared with those of the technetium and rhenium oxo complexes we reported earlier, thereby drawing group trends in the reactions of this important class of oxidation catalysts. In the reactions of MnO_3L (L = O^-, Cl^-, CH_3, OCH_3, Cp, NPH_3) with ethylene, it was found that the formation of the dioxylate intermediate along the concerted [3 + 2] addition pathway on the singlet potential energy is favored kinetically and thermodynamically over its formation by a two-step process *via* the metallaoxetane by [2 + 2] addition. The activation barriers for the formation of the dioxylate and the product stabilities on the singlet PES for the ligands studied are found to follow the order: $NPH_3 < Cl^- < CH_3O^- < Cp < O^- < CH_3$. On the doublet PES, the activation barriers for the formation of the dioxylate intermediate for the ligands are found to follow the order: $CH_3O^- < Cl^- < Cp < CH_3$ while the order of product stabilities is: $Cl^- < CH_3O^- < Cp < CH_3$. The order of dioxylate product stabilities on the triplet surface for the ligands studied is: $Cl^- < CH_3O^- < Cp < CH_3 < NPH_3 < O^-$ and the order on the quartet surface is $O^- < Cp < CH_3 < NPH_3 < Cl^- < CH_3O^-$. The re-arrangement of the metallaoxetane intermediate to the dioxylate is not a feasible reaction for all the ligands studied. Of the group VII B metal oxo complexes studied, MnO_4^- and $MnO_3(OCH_3)$ appear to be the best catalysts for the exclusive formation of the dioxylate intermediate, $MnO_3(OCH_3)$ being better so on both kinetic and thermodynamic grounds. The best epoxidation catalyst for the Mn complexes is MnO_3Cl; the formation of the epoxide precursor will not result from the reaction of $LMnO_3$ (L = O^-, Cp) with ethylene on any of the surfaces studied. The trends observed for the oxidation reactions of the Mn complexes with ethylene compare closely with those reported by us for the ReO_3L and TcO_3L (L = O^-, Cl, CH_3, OCH_3, Cp, NPH_3) complexes, but there is far greater similarity between the Re and Tc complexes than between Mn and either of the other two. There does not appear to be any singlet–triplet or doublet–quartet spin-crossover in any of the pathways studied.

Received 25th June 2013,
Accepted 1st August 2013

DOI: 10.1039/c3dt51700d

www.rsc.org/dalton

1. Introduction

Transition metal-oxo compounds and oxo-halides such as CrO_2Cl_2, OsO_4, MnO_4, ReO_4^- and RuO_4^- are applied extensively in reactions in which oxygen is inserted into C–H bonds or undergoes addition to an olefinic double bond. The application of such reagents in chemical synthesis has spurred considerable interest in the underlying reaction mechanism.[1–4]

Some transition metal-oxo complexes such as CrO_2Cl_2 react with olefins to form epoxides, chlorohydrins and vicinal dihalides[5,6] whereas others such as MnO_4^- and OsO_4 react to form diols without significant epoxide formation.[7,8] Many experimental and theoretical investigations have focused on mechanistic aspects of this type of reaction. Olefin dihydroxylation catalyzed by transition metal oxo species of the type MO_3L has been the subject of extensive theoretical studies.[9–17]

The mechanism of oxidation of alkenes by permanganate is believed to be related to the oxidation of alkenes by OsO_4, even though the reaction rates are influenced differently by donor and acceptor olefins on going from OsO_4 to MnO_4^- due to charge differences. The proposal that the initial step of the dihydroxylation reaction catalyzed by transition metal oxo compound MnO_4^- involves a direct [3 + 2] reaction of ethylene with the O═Mn═O group of MnO_4^- to form a metalladioxolane, a five-membered metallacycle[18] (structure **2** in Scheme 1), was generally favored, until Sharpless *et al.*[19] suggested a stepwise mechanism involving a metallaoxetane intermediate in the chromyl chloride oxidation. However, the

Department of Chemistry, Kwame Nkrumah University of Science and Technology, Kumasi, Ghana. E-mail: albertaniagyei@yahoo.com, richtiagh@yahoo.com, eadei@yahoo.com

†Electronic supplementary information (ESI) available. See DOI: 10.1039/c3dt51700d

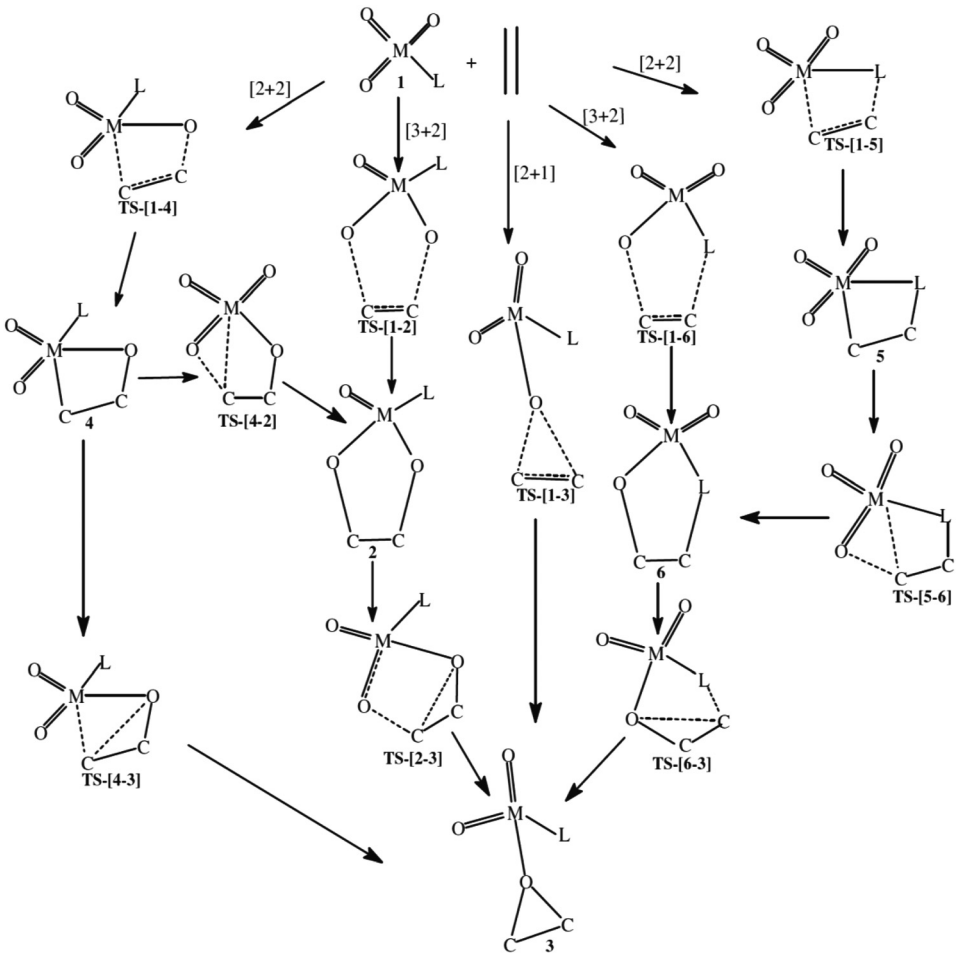

Scheme 1 Possible concerted pathways for the reaction of $LMnO_3$ (L = O^-, Cp, CH_3, CH_3O^-, NPH_3, Cl^-) with ethylene.

intermediacy of a metallaoxetane (structure **4** in Scheme 1) arising from the [2 + 2] addition pathway as suggested by Sharpless *et al.* for chromyl chloride oxidation was ruled out, at least for MnO_4^-, by density functional theory (DFT) calculations by Houk *et al.*[16] and corroborated by experimental kinetic isotope effect studies.[12,20]

For tetramethylethylene (TME) addition to MnO_3Cl, Limberg and Wistuba[21] reported the [3 + 2] addition of TME to the MnO_2 moiety of MnO_3Cl to be thermodynamically favored over the direct [2 + 1] addition (epoxidation) product while the kinetic barriers for both reactions were of comparable height at the B3LYP LANL2DZ/6-311G(d) level of theory. However, in an experimental investigation of the TME–MnO_3Cl system by means of matrix-isolation techniques, selective formation of the epoxidation product $ClO_2MnO[C(CH_3)_2]_2$ was observed. Limberg and Wistuba[21] did not find a minimum corresponding to the geometry of singlet or triplet metallaoxetane arising from the [2 + 2] addition pathway.

Strassner and Busold[22] found the activation barrier for the [3 + 2] addition pathway to be lower than the [2 + 2] addition pathway for permanganate oxidation of substituted alkynes, although the lowest lying identified state is a reactive triplet intermediate.

Theoretical calculations focusing on the [3 + 2] addition pathway were explored for the transition metal-oxo complex of the type CH_3MnO_3 with ethylene by Gisdakis and Rösch.[23] They found the activation barrier and reaction energy along the [3 + 2] route to be lower than the corresponding [2 + 2] addition pathway employing the hybrid B3LYP functional with effective core potentials and double-zeta basis sets, LanL2DZ, for the transition metal and 6-311G(d,p) basis sets for H, C, O, and F.

Strassner and Busold[24] reported the results of density functional theory calculations at the B3LYP/6-31G(d) level that strongly favor the [3 + 2] against the [2 + 2] addition pathway through a metallaoxetane intermediate for permanganate oxidation of substituted alkenes. The activation barriers associated with the [2 + 2] addition pathway are very high (61.5–67.3 kcal mol^{-1}). The metallaoxetane intermediates were calculated to be endothermic with reaction energies between +24.7 and +33.6 kcal mol^{-1}. The endothermic formation of the metallaoxetane product *via* the [2 + 2] transition state that is on average 40 kcal mol^{-1} higher in energy is not competitive with the [3 + 2] addition pathway which has a lower activation barrier (10.8–14.7 kcal mol^{-1}) which leads to exothermic products.

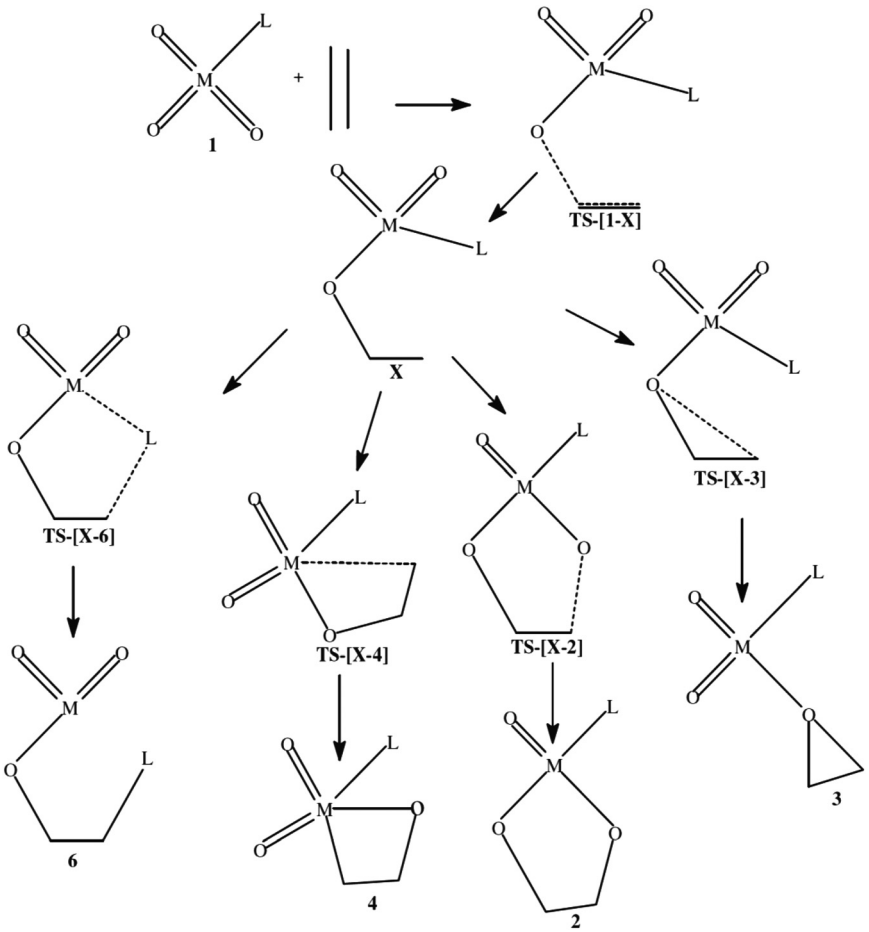

Scheme 2 Possible stepwise pathway for the reaction of $LMnO_3$ (L = O^-, Cl^- CH_3O–, CH_3, Cp, NPH_3) with ethylene.

Aniagyei, Tia and Adei studied the mechanisms of oxidation of ethylene with ReO_3L (L = O^-, Cl^-, Cp, CH_3, OCH_3, NPH_3)[25] and TcO_3L (L = O^-, Cl^-, Cp, CH_3, OCH_3, NPH_3).[26] It was found that on the singlet surface the [3 + 2] addition leading to the formation of the dioxylate intermediate was the predominantly favored pathway for both the Re and Tc complexes, with the activation barriers being in the order O^- > CH_3 > NPH_3 > CH_3O^- > Cl^- > Cp for both metals. It was also found that for the Re system the best dioxylating catalyst is ReO_3Cp (singlet surface) while the best epoxidation catalyst is ReO_3Cl (singlet surface); and for the Tc system the best dioxylating catalyst is TcO_3Cp (singlet surface) while the best epoxidation catalyst is TcO_3Cl (singlet surface); thus the Cp ligand gave the best dioxylating catalyst in both metals while the Cl^- ligand gave the best epoxidation catalyst in both metals. The ReO_4^-, ReO_3Cp, TcO_4^- and TcO_3Cp reaction surfaces were found to be much 'cleaner' than the rest of the complexes studied, *i.e.* there are no side-reactions competing with the formation of the dioxylate and metallaoxetane intermediates with the O^- and Cp ligands for both metals.

In this work, the potential energy surfaces for the oxidation of ethylene by MnO_3L (L = O^-, Cl^-, Cp, CH_3, OCH_3, NPH_3) are explored with hybrid density functional theory at the B3LYP/LACVP* level of theory. The [3 + 2] and [2 + 2] addition pathways to form metallaoxetanes and dioxylates, the conversion of the metallaoxetanes to the dioxylates and the formation of epoxide precursors (Schemes 1 and 2) are investigated. The results are discussed and compared with the oxidations of ethylene with the ReO_3L and TcO_3L (L = O^-, Cl^-, Cp, CH_3, OCH_3, NPH_3) systems in order to explore group trends in the reactions. Multiple spin states have been considered in the calculations. Organometallic reactions are known to occur on more than one spin surface;[27–29] many reactions involve several states of different spins.[30] A change of spin state can affect the molecular structure in terms of bond lengths, angular distortions and even overall molecular geometry[31] and spin crossing effects can dramatically affect reaction mechanisms of organometallic transformations.[32]

2. Details of calculations

All calculation were carried out using Spartan'08 V1.2.0 and Spartan'10 V1.1.0 Molecular Modeling programs[33] at the DFT

B3LYP/LACVP* level of theory. The B3LYP functional is a Hartree–Fock DFT hybrid functional. The LACVP* basis set is a relativistic effective core-potential that describes the atoms H–Ar with the 6-31G* basis while heavier atoms are modeled with the LANL2DZ basis set which uses the all-electron valence double zeta basis set (D95 V), developed by Dunning, for first row elements[34] and the Los Alamos ECP plus double zeta basis set developed by Wadt and Hay for the atoms Na–La, Hf–Bi.[35–37]

The starting geometries of the molecular systems were constructed using Spartan's graphical model builder and minimized interactively using the sybyl force field.[38] All geometries were fully optimized without any symmetry constraints. A normal mode analysis was performed to verify the nature of the stationary point. Equilibrium geometries were characterized by the absence of imaginary frequencies.

The transition state structures were located by a series of constrained geometry optimizations in which the forming- and breaking-bonds were fixed at various lengths while the remaining internal co-ordinates were optimized. The approximate stationary points located from such a procedure were then fully optimized using the standard transition state optimization procedure in Spartan. All first-order saddle points were shown to have a Hessian matrix with a single negative eigenvalue, characterized by an imaginary vibrational frequency along the reaction coordinate.

For the MnO_3Cl, $MnO_3(CH_3)$, $MnO_3(OCH_3)$, MnO_3Cp and $MnO_3(NPH_3)$ systems, the singlet and triplet species were computed as neutral structures while the doublet and quartet species were computed as anions. For the TcO_4^- system, the singlet and triplet species were computed as anions while the doublet and quartet species were computed as neutral structures.

3. Results and discussion

3.1. Reaction of MnO_4^- with ethylene

The relative energies of the main stationary points involved in the reactions between MnO_4^- and ethylene are shown in Fig. 1. (The full set of optimized structures for all the systems herein reported is shown in Fig. S1–S6 in the ESI†). The density functional theory (DFT) optimization of the MnO_4^- reactant shows that the MnO_4^- can have a singlet ground state electronic structure (**A1/s**), a doublet electronic ground state structure, a triplet ground state electronic structure and a quartet ground state electronic structure. The Mn–O bond length of the singlet structure is 1.60 Å, which is in agreement with the experimentally-determined X-ray data on permanganate.[39] The triplet reactant is 22.4 kcal mol^{-1} less stable than the singlet and the doublet reactant is 23.2 kcal mol^{-1} more stable than the quartet.

On the singlet PES, the [3 + 2] addition of the C═C π bond of ethylene across the O═Mn═O bonds through transition state **TS-[A1-A2]/s** to form dioxomangana-2,5-dioxolane **A2/s** has an activation barrier of 9.14 kcal mol^{-1} and an exothermicity of 47.6 kcal mol^{-1}, in agreement with the work of Houk *et al.*[16] who computed the barrier for this route to be 9.2 kcal mol^{-1}, with a reaction energy of −47.2 kcal mol^{-1} at the B3LYP level of theory.

A triplet dioxomangana-2,5-dioxolane was found to be 2.1 kcal mol^{-1} more stable than the singlet dioxylate but no triplet [3 + 2] transition state could be located. A quartet dioxylate species was found but no doublet dioxylate product could be located on the reaction surface. No doublet or quartet transition states could also be located.

In a related study on the osmium tetraoxide reaction with ethylene, Tia and Adei[40] found the activation barrier for the

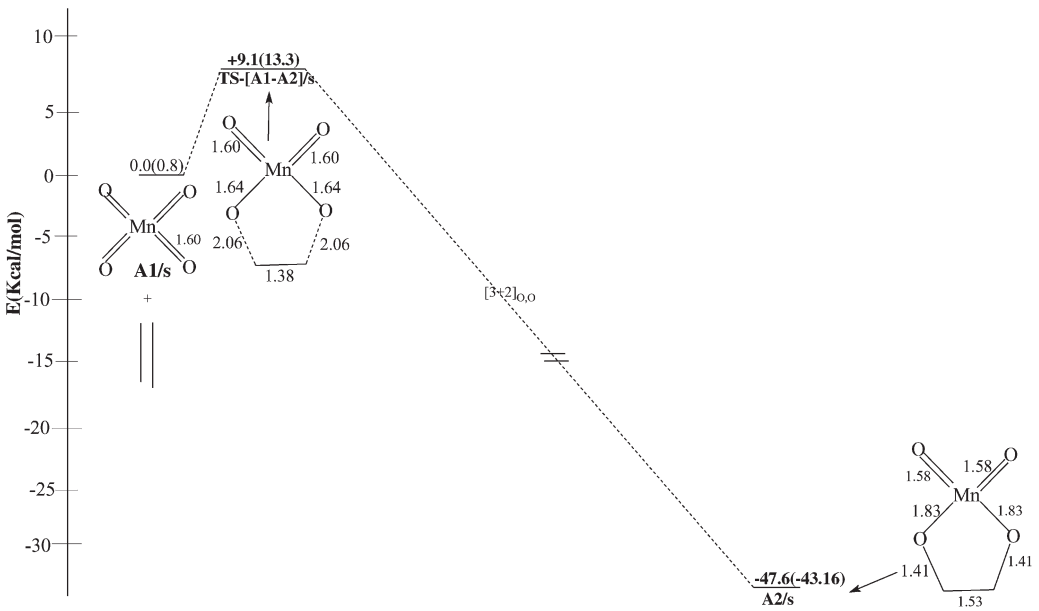

Fig. 1 Energetics of the reaction of MnO_4^- with ethylene. Energies with zero point corrections in parentheses.

[3 + 2] addition to form the osmadioxylate ester intermediate to be very low (3.97 kcal mol^{-1}). Earlier studies by Frenking *et al.*,[41] Ziegler *et al.*[42] and Morokuma *et al.*[43] reported similar findings. The calculated barrier for the [3 + 2] addition of the C═C bond of ethylene across the O═Os═O bonds of OsO_4 is much lower than the barrier calculated for the MnO_4^- (9.1 kcal mol^{-1}) in this work, an analogous reaction of isoelectronic OsO_4.

The formation of the singlet manganooxetane **A3/s** by [2 + 2] addition of the C═C bond of ethylene across the M═O bond of the permanganate complex **A1** is 18.5 kcal mol^{-1} endothermic, in agreement with the value reported by the study of Houk *et al.*[16] at the B3LYP level of theory. A triplet metallaoxetane was located and was found to be 7.1 kcal mol^{-1} less stable than the singlet **A3/s**. The doublet manganooxetane is 14.5 kcal mol^{-1} less stable than the quartet metallaoxetane species, but no doublet, triplet or quartet transition states could be located.

The re-arrangement of the manganooxetane to the dioxylate (**TS-[4-2]** in Scheme 1) as suggested by Sharpless *et al.*[19] for the chromyl chloride oxidation of olefins was also explored for the reaction of permanganate with ethylene. The activation barrier for the re-arrangement of the singlet manganooxetane to the dioxylate is 28.1 kcal mol^{-1}. No transition state was located for the re-arrangement of the triplet manganooxetane to the dioxylate. The overall activation barrier for the re-arrangement of the singlet manganooxetane to the dioxylate is higher than the activation barrier for the direct [3 + 2] addition of ethylene across the two oxygen atoms of singlet MnO_4^-.

The potential energy surface of the reaction of permanganate with ethylene was further explored in an attempt to locate an epoxide precursor (O_3–Mn–OC_2H_4) (**3** in Scheme 1), but no such minimum was found on the reaction surface. From the work of Ziegler *et al.*[42] and Tia and Adei[44] and Scheme 1, the epoxide precursor could be formed from re-arrangement of the five-membered metallacycle through transition state **TS-[6-3]**, re-arrangement of the metalladioxolane through transition state **TS-[2-3]**, re-arrangement of the metallaoxetane through transition state **TS-[4-3]** or from direct [2 + 1] addition through transition state **TS-[1-6]**. None of these transition states were found, indicating that the reaction of ethylene with MnO_4^- does not lead to the formation of the epoxide precursor. Thus the oxidation of ethylene with MnO_4^- will form exclusively diols.

3.2. Reaction of MnO_3Cl with ethylene

The energy profile of the reaction between MnO_3Cl and ethylene and some of the optimized structures in the reaction are shown in Fig. 2 and 3. The DFT geometry optimization of MnO_3Cl on a singlet potential energy surface (PES) yielded two minima: **R1-A4/s** of C_{3V} symmetry and **R2-A4/s** of C_S symmetry in which the Mn–Cl bond is broken and the chloro is bonded to one of the oxo ligands. Doublet, triplet and quartet reactants were also located. The structure **R1-A4/s** has been

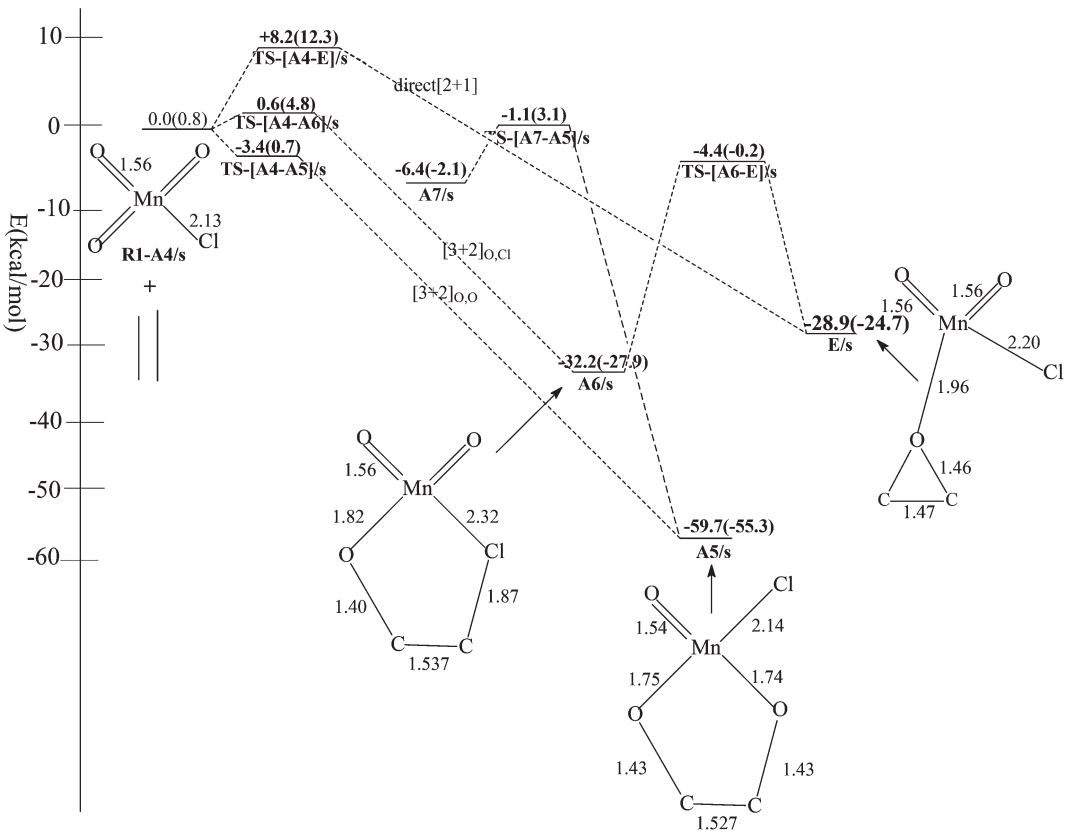

Fig. 2 Energetics of the reaction of MnO_3Cl with ethylene on the singlet PES. Energies with zero point corrections in parentheses.

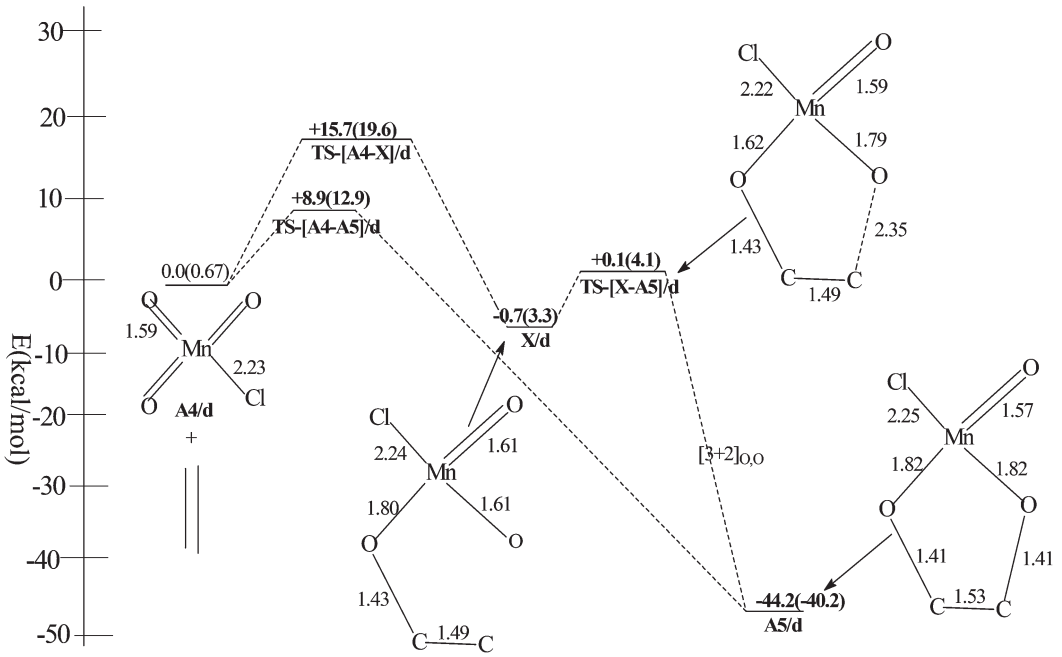

Fig. 3 Energetics of the reaction of MnO_3Cl with ethylene on the doublet PES. Energies with zero point corrections in parentheses.

computed to be 36.6 kcal mol^{-1} more stable than **R2-A4/s** and 24.4 kcal mol^{-1} more stable than the triplet reactant. The doublet reactant has been found to be 17.8 kcal mol^{-1} more stable than the quartet reactant.

As seen in Fig. 2, the activation barrier for the direct [3 + 2] addition of ethylene across the two oxygen atoms of MnO_3Cl to form the dioxylate intermediate on the singlet PES through the singlet transition state **TS-[A4-A5]/s** is barrierless, with a reaction energy of −59.7 kcal mol^{-1}. The [3 + 2] addition of the C═C π bond of ethylene across the O═Mn–Cl bonds of MnO_3Cl on the singlet surface through the transition state **TS-[A4-A6]/s** has an activation barrier of 0.64 kcal mol^{-1} and a reaction energy of −32.2 kcal mol^{-1}.

The formation of the singlet manganooxetane through [2 + 2] addition of the C═C bond of ethylene across the Mn═O bond of singlet permanganyl chloride complex **R1-A4** has a reaction energy of 1.5 but no transition could be located for this step. The activation barrier for the re-arrangement of metallaoxetane **A7/s** through the singlet transition state **TS-[A7-A5]/s** to the dioxylate was found to be 5.3 kcal mol^{-1}. This barrier is higher than that for the direct [3 + 2] addition across the two oxygen atoms of singlet MnO_3Cl.

An epoxide precursor formation was explored for the reaction of MnO_3Cl with ethylene; this was unsuccessful in the case of MnO_4^-. The transition state **TS-[A6-E]/s** for the re-arrangement of the singlet five-membered metallacycle (**TS-[1-6]** in Scheme 1) to the epoxide precursor has an activation barrier of 27.8 kcal mol^{-1} and an endothermicity of +3.3 kcal mol^{-1}. The activation barrier and reaction energy for the direct [2 + 1] one-step addition of the C═C bond across one oxygen atom of MnO_3Cl on the singlet PES through transition state **TS-[A4-E]/s** are 8.2 and −28.9 kcal mol^{-1}. Thus the epoxide precursor will most likely arise from a direct [2 + 1] addition.

On the doublet PES (Fig. 3), the [3 + 2] addition of the C═C π bond of ethylene across the O═Mn═O bonds of doublet MnO_3Cl was found to follow either the concerted or stepwise (Scheme 2) addition pathways. On the concerted pathway, the activation barrier for the formation of the dioxylate species **A5/d** is 8.9 kcal mol^{-1}. The dioxylate species **A5/d** has an exothermicity of 44.2 kcal mol^{-1}. Along the stepwise pathway, one of the C═C π bonds of ethylene attacks an oxo-ligand of MnO_3Cl to form the organometallic intermediate **X/d** (**X** in Scheme 2). The activation barrier for the formation of the intermediate **X/d** is 15.7 kcal mol^{-1}. The intermediate **X/d** has an exothermicity of 0.6 kcal mol^{-1}. The intermediate can then rearrange through transition state **TS-[X-A5]/d** to form the dioxylate **A5/d** with an activation barrier of 0.7 kcal mol^{-1}. A quartet species **A5/q** has been computed to be 28.1 kcal mol^{-1} more stable than the doublet product **A5/d**.

The formation of the doublet manganooxetane through [2 + 2] addition of the C═C bond of ethylene across the Mn═O bond of doublet permanganyl chloride complex **R1-A4** has a reaction energy of 6.4 kcal mol^{-1} but no transition state for this step could be located.

A quartet metallaoxetane-like species **A7/q** but with an elongated metal–carbon bond has been found and has an exothermicity of 18.13 kcal mol^{-1}. The formation of the metallaoxetane **A7** could potentially have come from intermediate **X/d** and **A7/q**; however attempts at locating the relevant transition states linking the intermediate to the metallaoxetane were not successful. No triplet metallaoxetane intermediate **A9/t** was located on the triplet reaction surface.

3.3. Reaction of $MnO_3(NPH_3)$ with ethylene

Fig. 4 shows the main stationary points involved in the reaction between $MnO_3(NPH_3)$ and ethylene and some of the optimized structures. The $MnO_3(NPH_3)$ reactant was found to have singlet, doublet and triplet structures. However, unlike the singlet and triplet which are open structures, the doublet has a ring with Mn–N–P–O ring closure (see ESI†).

On the singlet PES, the [3 + 2] addition of the C═C bond of ethylene across the O═Mn═O bonds of singlet $MnO_3(NPH_3)$ through transition state **TS-[A8-A9]/s** to form the dioxylate intermediate **A9/s** is barrierless and has a reaction energy of −60.4 kcal mol^{-1}. A triplet dioxylate has been found to be 22.9 kcal mol^{-1} more stable than the singlet. No corresponding transition state linking the reactants to the products could be located on the doublet PES. However, a doublet dioxylate product was found to be 7.1 kcal mol^{-1} less stable than the quartet dioxylate product.

The [3 + 2] addition of the C═C bond of ethylene across the O═Mn═N bonds of singlet $MnO_3(NPH_3)$ through the singlet transition state **TS-[A8-A10]/s** to form intermediate **A10/s** is also barrierless and has a reaction energy of −65.3 kcal mol^{-1}. On the doublet, triplet and quartet surfaces, seven-membered intermediates have been located which correspond to structure **A9/s** but with an additional bond between one of the oxo ligands on the metal center and a phosphine attached to the nitrogen in the five-membered ring of **A9/s**. The triplet is 2.3 kcal mol^{-1} more stable than the singlet while the quartet structure is 16.7 kcal mol^{-1} less stable than the doublet.

The metallaoxetanes located on the singlet, doublet, triplet and quartet reaction surfaces have a bond between the phosphine P atom and the ring O atom (**A12/s**, **A12/d**, **A12/t** and **A12/q** in ESI†). The triplet species is 10.6 kcal mol^{-1} more stable than the singlet and the doublet structure is computed to be 0.8 kcal mol^{-1} less stable than the quartet species. However, no transition state could be located linking the reactants to these structures. The formation of a singlet metallacyclic intermediate **A11/s** through transition state **TS-[A8-A11]/s** (Fig. 4) by [2 + 2] addition of the C═C π bond of ethylene across the Mn═N bond of the singlet $MnO_3(NPH_3)$ has an activation barrier of 17.6 kcal mol^{-1} and leads to a six-membered product in which one of the oxo groups on the metal centre bonds with a P atom (1.78 Å). The singlet product has an exothermicity of 27.4 kcal mol^{-1}. A triplet species has a reaction energy of −14.7 kcal mol^{-1}. This six-membered product was found to have doublet, triplet and quartet counterparts but there are no corresponding doublet, triplet and quartet transition states. The doublet species is 3.6 kcal mol^{-1} more stable than the quartet species.

A search of the surfaces for the re-arrangement of the four membered metallacycle metallaoxetane to the five membered metallacycle was unsuccessful.

The reaction of $MnO_3(NPH_3)$ with ethylene was explored for the possibility of formation of an epoxide precursor. The rearrangement of the singlet five-membered metallacycle through transition state **TS-[A10-E]/s** (*i.e.* **TS-[1-6]** in Scheme 1) to the epoxide precursor has an activation barrier of 63.1 kcal mol^{-1}

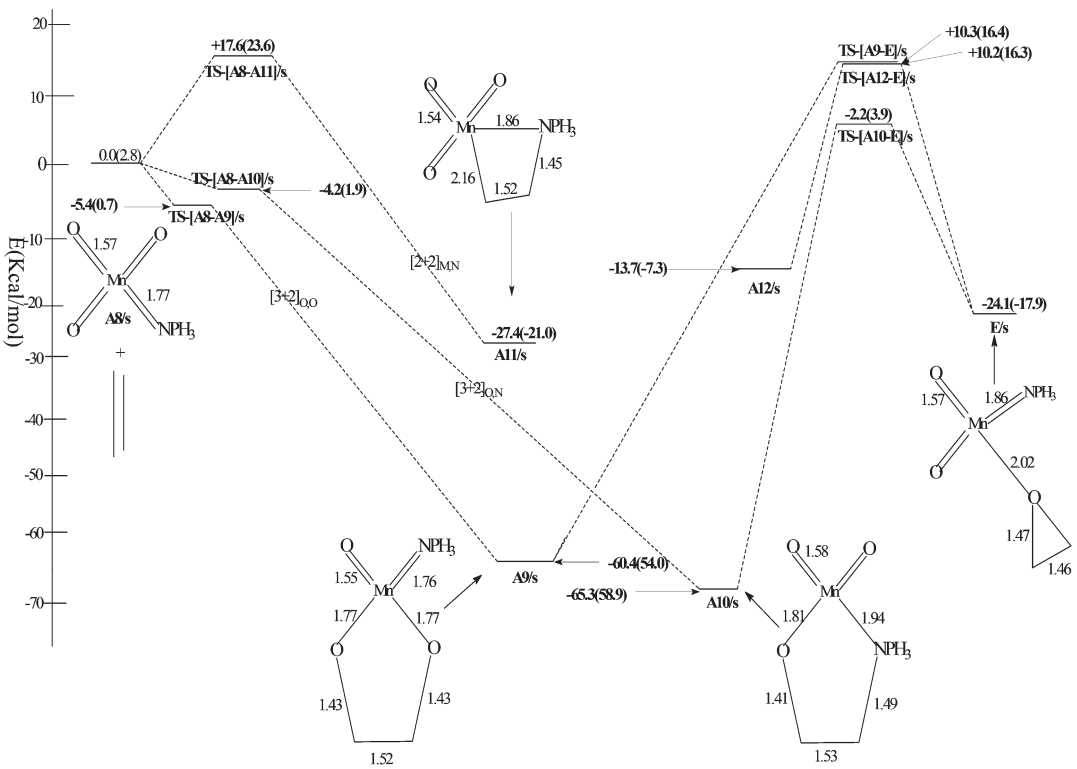

Fig. 4 Energetics of the reaction of $MnO_3(NPH_3)$ with ethylene. Energies with zero point corrections in parentheses.

and a reaction energy of +41.2 kcal mol^{-1}. Also the re-arrangement of the singlet five-membered metallacycle (**TS-[2-3]** in Scheme 1) through transition state **TS-[A9-E]/s** to the epoxide precursor has an activation barrier of 70.7 kcal mol^{-1} and an endothermicity of +36.4 kcal mol^{-1}. The re-arrangement of the singlet four-membered metallaoxetane to the epoxide precursor has a barrier of 23.9 kcal mol^{-1} and an exothermicity of 10.4 kcal mol^{-1}. However since the activation energy required to form the metallaoxetane is not known, no conclusion could be drawn on the formation of the epoxide precursor for the metallaoxetane.

3.4. Reaction of $MnO_3(CH_3)$ with ethylene

The optimized geometries and the energy profile of the reaction of $MnO_3(CH_3)$ with ethylene are shown in Fig. 5. On the singlet surface, two minima correspond to the formula $MnO_3(CH_3)$: **R1-A13** of C_{3V} symmetry and **R2-A13** of C_1 symmetry in which the methyl ligand breaks from the metal centre and forms a new bond with one of the oxo-ligands. Structure **R2-A13** is 11.81 kcal mol^{-1} more stable than **R1-A13**. A doublet reactant **A13/d** has been found to be 26.0 kcal mol^{-1} more stable than the quartet species **A13/q**. (Structures **R2-13**, **A13/d** and **A13/q** are shown in the ESI†.)

On the singlet surface, the activation barrier for the [3 + 2] addition of the C═C π bond of ethylene across the O═Mn═O bonds of singlet $MnO_3(CH_3)$ through transition state **TS-[A13-A14]/s** has an activation barrier of 20.3 kcal mol^{-1} and a reaction energy of −25.9 kcal mol^{-1}. The singlet dioxylate is 30.0 kcal mol^{-1} more stable than the triplet dioxylate.

On the doublet PES, the [3 + 2] addition of the C═C π bond of ethylene across the O═Mn═O bonds of doublet $MnO_3(CH_3)$ through a doublet transition state **TS-[A13-A14]/d** to form the dioxylate **A14/d** has an activation barrier of 15.9 kcal mol^{-1} and a reaction energy of −29.7 kcal mol^{-1}. A quartet dioxylate **A14/q** is 36.7 kcal mol^{-1} more stable than the doublet product **A14/d**.

The formation of singlet manganooxetane **A15/s** by [2 + 2] addition of the C═C bond of ethylene across the Mn═O bond of $MnO_3(CH_3)$ through the singlet transition state **TS-[A13-A15]/s** has an activation barrier of 51.4 kcal mol^{-1} and a reaction energy of +9.1 kcal mol^{-1}. The formation of the doublet manganooxetane **A15/d** through doublet transition state **TS-[A13-A15]/d** has an activation barrier of 18.4 kcal mol^{-1} and a reaction energy of +13.9 kcal mol^{-1}. A triplet metallaoxetane intermediate has been computed to be 38.8 kcal mol^{-1} more stable than the singlet **A15/s** metallaoxetane intermediate while a quartet metallaoxetane species has been computed to be 7.29 kcal mol^{-1} more stable than the doublet metallaoxetane intermediate. No quartet transition state linking the reactants to the products could be located on the reaction surface.

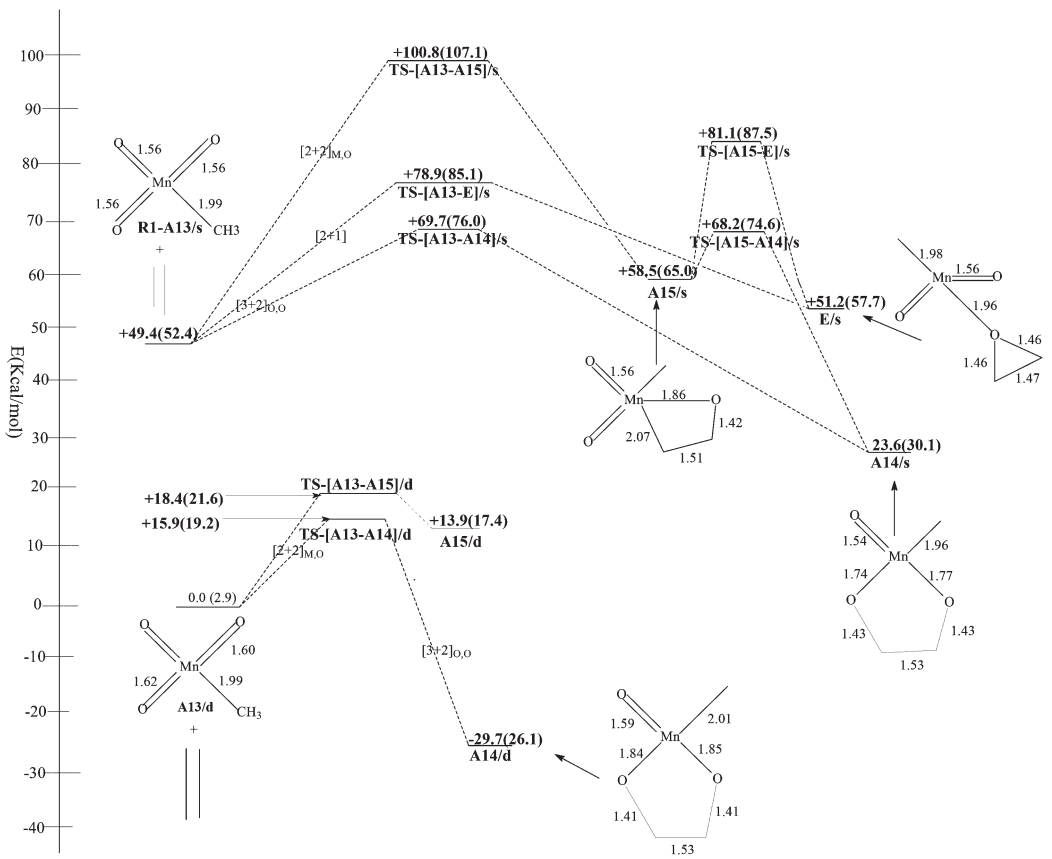

Fig. 5 Energetics of the reaction of $MnO_3(CH_3)$ with ethylene. Energies with zero point corrections in parentheses. Note that the singlet structures and the doublet structures are not isoelectronic and therefore their energies are not to be compared directly.

The re-arrangement of the singlet metallaoxetane to the singlet dioxylate through transition state **TS-[A15-A14]/s** has an activation barrier of 18.8 kcal mol^{-1}. Even though the overall activation barrier for the re-arrangement of the singlet metallaoxetane to the dioxylate is lower than the activation barrier for the direct [3 + 2] addition of C═C π of ethylene across the O═Mn═O bonds of singlet and doublet $MnO_3(CH_3)$, the formation of the metallaoxetane from which the re-arrangement occurs has a higher activation barrier; the dioxylate would most likely proceed from the direct [3 + 2] addition pathway and not from the metallaoxetane through the [2 + 2] addition pathway.

The formation of an epoxide precursor was explored from the reaction of $MnO_3(CH_3)$ with ethylene. The re-arrangement of the singlet metallaoxetane to the epoxide precursor through transition state **TS-[A15-E]/s** has an activation barrier and a reaction energy of 22.52 and −7.32 kcal mol^{-1} respectively. Also, the activation energy for the formation of the singlet epoxide precursor from direct attack of the C═C bond across the oxygen atom of $MnO_3(CH_3)$ has been computed to be 29.45 kcal mol^{-1}, with a reaction energy of +1.8 kcal mol^{-1}. On the doublet, triplet, and quartet surfaces, the epoxide precursor has been computed to have reaction energies of +4.6, −40.6 and −21.5 kcal mol^{-1} respectively. The most plausible pathway for the formation of the epoxide precursor is by the direct [2 + 1] addition pathway on the singlet PES.

The oxidation of ethylene with $MnO_3(CH_3)$ will most likely lead to the formation of diols, albeit with a high activation barrier.

3.5. Reaction of $MnO_3(OCH_3)$ with ethylene

The optimized geometries and relative energies of the main stationary points involved in the reaction between $MnO_3(OCH_3)$ and ethylene are shown in Fig. 6. Singlet, doublet, triplet and quartet species have been optimized for the reactant $MnO_3(OCH_3)$. The doublet reactant is 20.24 kcal mol^{-1} more stable than the quartet species while the triplet structure is 20.25 kcal mol^{-1} less stable than the singlet structure.

On the doublet surface, there is a stepwise attack of one of the C═C π of ethylene on an oxo-ligand of $MnO_3(OCH_3)$ to form an organometallic intermediate **X/d** through transition state **TS-[A16-X]/d**. The activation barrier along this route is 3.28 kcal mol^{-1}. The intermediate **X/d** is 0.63 kcal mol^{-1} less stable than the separated reactants. The intermediate **X/d** then re-arranges through transition state **TS-[X-A17]/d** to form the

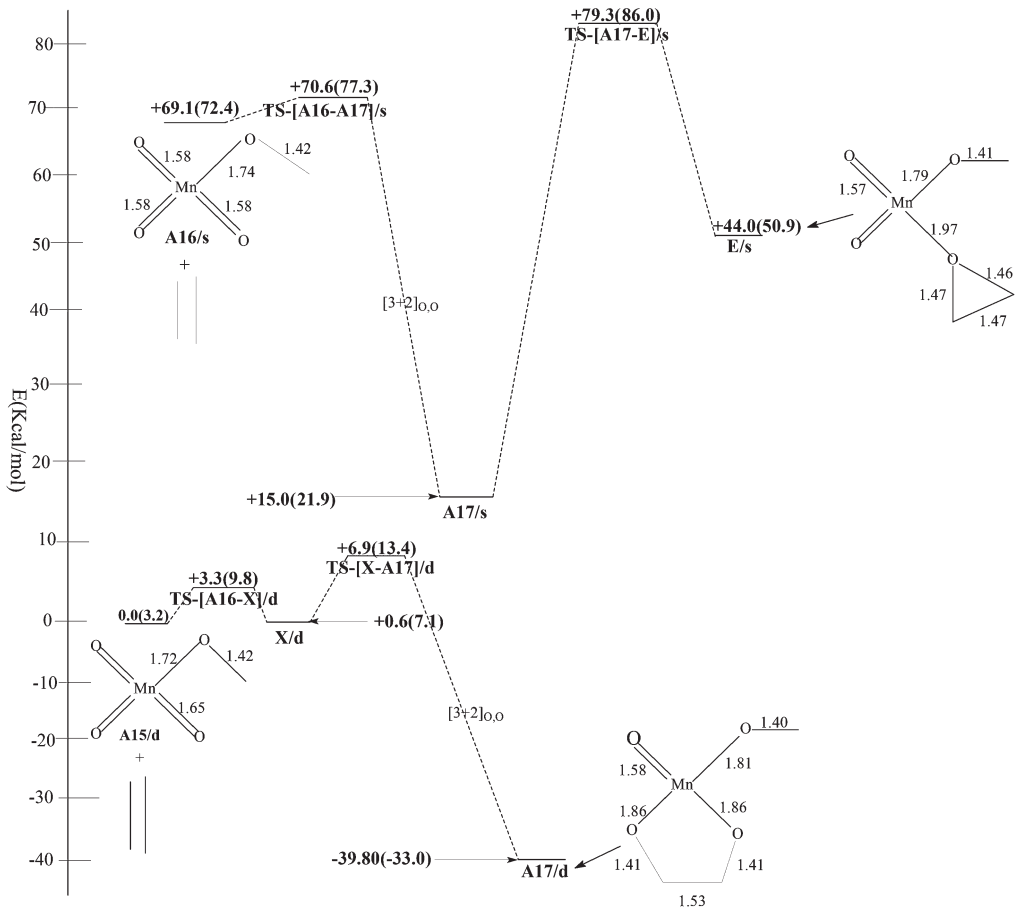

Fig. 6 Energetics of the reaction of $MnO_3(OCH_3)$ with ethylene. Energies with zero point corrections in parentheses. Note that the singlet structures and the doublet structures are not isoelectronic and therefore their energies are not to be compared directly.

dioxylate intermediate **A17/d**, a reaction that has a barrier of 6.26 kcal mol^{-1} and a reaction energy of −39.80 kcal mol^{-1}. A quartet product **A17/q** has been computed to have a reaction energy of +26.48 kcal mol^{-1}.

The activation barrier for the direct [3 + 2] addition of ethylene across the O═Mn═O bonds of singlet $MnO_3(OCH_3)$ through a singlet transition state **TS-[A16-A17]/s** to form dioxylate intermediate **A17/s** is 1.6 kcal mol^{-1}, with a reaction energy of −54.1 kcal mol^{-1}. A triplet dioxylate was located and found to be 34.3 kcal mol^{-1} more stable than the singlet dioxylate product.

Attempts at locating the manganooxetane product which is expected to result from the [2 + 2] addition of ethylene to the Mn═O bonds of singlet and doublet $MnO_3(OCH_3)$ proved unsuccessful.

The reaction of $MnO_3(OCH_3)$ with ethylene was explored for the formation of the epoxide precursor. The re-arrangement of the five-membered dioxylate through transition state **TS-[A17-E]/s** to the epoxide precursor has an activation barrier of 64.3 kcal mol^{-1} and a reaction energy of +29.1 kcal mol^{-1}.

Therefore, the most plausible pathway for the formation of the epoxide precursor is by initial [3 + 2] addition across the two oxygen atoms of singlet $MnO_3(OCH_3)$ followed by re-arrangement to the epoxide precursor.

Thus in the reaction of $MnO_3(OCH_3)$ with ethylene, the reaction will preferentially take place on the singlet surface and the [3 + 2] addition of ethylene across the two oxygen atoms of $MnO_3(OCH_3)$ to form the dioxylate intermediate is kinetically and thermodynamically the most favored. The energetics as shown in Fig. 6 preclude the formation of an epoxide.

3.6. Reaction of MnO_3Cp with ethylene

Fig. 7 shows the optimized geometries and relative energies of the main stationary points involved in the reaction between MnO_3Cp and ethylene. Singlet, doublet, triplet and quartet reactants have been optimized. In the singlet reactant **A18/s**, the cyclopentadienyl ligand Cp is bonded in a η^3 fashion in the singlet reactant, *i.e.* Mn–C (Cp) = (2.018, 2.838 and 2.830 Å). Gisdakis and Rösch[23] reported the Cp ligand to be bonded in a η^1 fashion to the metal centre in MnO_3Cp at B3LYP LANL2DZ/6-311G(d,p) level of theory. A doublet reactant has been computed to be 24.2 kcal mol^{-1} more stable than the quartet reactant. The cyclopentadienyl ligand is bonded in a η^3 fashion to the Mn in the doublet reactant, *i.e.* Mn–C (Cp) = (2.04, 2.90, 2.92, 3.80 and 3.81 Å). In the triplet reactant, the cyclopentadienyl ligand is bonded to the manganese centre in a η^5 fashion, *i.e.* Mn–C (Cp) = (2.21, 2.26, 2.46, 2.46 and 2.26 Å). The triplet reactant is 21.05 kcal mol^{-1} less stable than

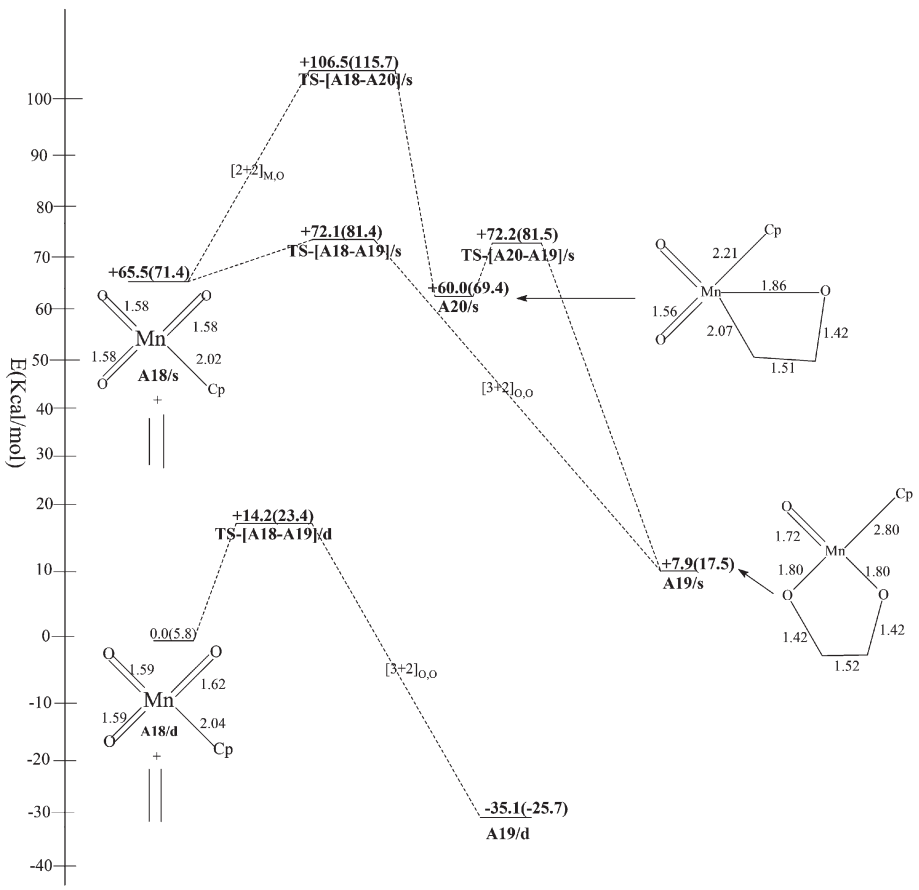

Fig. 7 Energetics of the reaction of MnO_3Cp with ethylene. Energies with zero point corrections in parentheses. Note that the singlet structures and the doublet structures are not isoelectronic and therefore their energies are not to be compared directly.

the singlet reactant. The cyclopentadienyl ligand is bonded in a η^3 fashion to the Mn in the quartet structure, *i.e.* Mn–C (Cp) = 2.05, 2.84, 2.89, 3.69 and 3.72 Å.

It has been found that the formation of the cyclic ester intermediate through the [3 + 2] addition pathway can proceed from a doublet as well as a singlet transition state. The activation barrier through the doublet transition state is 14.2 kcal mol^{-1} while the barrier through the singlet is 6.57 kcal mol^{-1}. The dioxylate intermediates have been found to be very stable. The singlet, doublet, triplet and quartet dioxylates are respectively 57.6, 35.1, 85.8 and 70.7 kcal mol^{-1} more stable than their respective separated reactants.

The Cp ligand in the singlet MnO_3Cp-dioxylate **A19/s** shows a η^5-bonding fashion to the Mn (Mn–C (Cp) = 2.22, 2.22, 2.33, 2.36, 2.26 Å) contrary to the η^3-bonded mode shown in the singlet reactant. A η^5-bonding mode (Mn–C (Cp) = 2.24, 2.27 and 2.29, 2.36, 2.34 Å) is also shown in the triplet product **A19/t**. The Cp ligand in the quartet MnO_3Cp-dioxylate **A19/q** shows a η^4-bonding fashion to the Mn centre (Mn–C (Cp) = 2.34, 2.33 and 2.82, 2.84 and 3.08 Å) contrary to the η^3-bonded mode expressed in the quartet reactant.

The formation of the singlet manganooxetane **A20/s** from the [2 + 2] addition of ethylene across the Mn=O bond of the singlet MnO_3Cp has an activation barrier of 40.9 kcal mol^{-1} through a singlet transition state **TS-[A18-A20]/s**. The manganooxetane is 5.5 kcal mol^{-1} below the reactants on the energy profile. The Cp ligand in the singlet MnO_3Cp-oxetane **A20/s** shows η^3-bonding mode to the Mn (Mn–C (Cp) = 2.12, 2.89, 2.96, 3.77 and 3.81 Å) in conformity with η^3-bonding mode in the singlet reactant. A triplet metallaoxetane intermediate has been found to be 62.0 kcal mol^{-1} more stable than the singlet metallaoxetane. The Cp ligand in the quartet MnO_3Cp-oxetane **A20/q** shows η^3-bonding mode to the Mn centre (Mn–C (Cp) = 2.09, 2.91 and 2.96, 3.79 and 3.82 Å).

No pathway was found for the re-arrangement of the metallaoxetane to the dioxylate on any of the surfaces studied.

The potential energy surface of the reaction of MnO_3Cp with ethylene was further explored in an attempt to locate an epoxide precursor [(Cp)O_2–Mn–OC_2H_4] (**3** in Scheme 1), but no such minimum was found on these reaction surfaces.

3.7. Comparison of the reactions of the manganese, technetium and rhenium oxo complexes with ethylene

Table 1 shows the activation barriers of the first step of the various reactions of the group VII B oxo complexes with ethylene for the various ligands studied in this work and in ref. 25 and 26.

It is seen from the table that for the O^-, Cp, OCH_3, and Cl^- ligands, the $[3 + 2]_{O,O}$ pathway is the most preferred pathway but the selectivity (in kinetic terms) decreases down the group. For example, for MnO_4^- the $[3 + 2]_{O,O}$ is the only pathway found; for TcO_4^- the $[3 + 2]_{O,O}$ activation barrier is about half the barrier of the $[2 + 2]_{M,O}$ pathway, the only other pathway found, while for ReO_4^- the activation barriers of the $[3 + 2]_{O,O}$ and $[2 + 2]_{Re,N}$ addition pathways are much closer.

Table 1 Activation barriers of the first step of the various reactions of the metal complexes

Metal		$-O^-$	$-Cl$	$-NPH_3$	$-CH_3$	$-OCH_3$	$-Cp$
Mn	$[3 + 2]_{O,O}$	9.1	−3.4	−5.4	69.7	1.5	6.6
	$[2 + 2]_{M,O}$	—	—	—	100.8	—	41.0
	$[3 + 2]_{L,O}$	—	0.6	—4.2	—	—	—
	$[2 + 1]$	—	8.2	—	78.9	—	—
	$[2 + 2]_{M,N}$	—	—	17.6	—	—	—
Tc[a]	$[3 + 2]_{O,O}$	24.2	7.6	15.4	19.83	13.1	2.7
	$[2 + 2]_{M,O}$	48.2	32.1	23.2	33.05	30.6	28.6
	$[3 + 2]_{L,O}$	—	14.7	16.6	—	—	—
	$[2 + 1]$	—	29.0	32.0	34.3	37.7	—
Re[b]	$[3 + 2]_{O,O}$	36.3	21.0	27.2	33.9	26.3	13.6
	$[2 + 2]_{M,O}$	46.7	29.6	41.7	47.7	30.6	33.0
	$[3 + 2]_{L,O}$	—	26.3	25.9	—	—	—
	$[2 + 1]$	—	—	52.9	56.5	60.4	—
	$[2 + 2]_{M,N}$	—	—	30.5	—	—	—

[a] Data from ref. 25. [b] Data from ref. 26.

The activation barriers for the $[3 + 2]_{O,O}$ addition increase from Mn through Tc to Re for all the ligands studied except for $-NPH_3$ and –Cp where the barriers for Mn are higher than those for Tc.

In the work reported, three transition states **TS-[A4-A5]/s**, **TS-[A8-A9]/s**, **TS-[A8-A10]/s** are below their respective reactants on the energy profiles, thereby giving slightly negative activation barriers for those reactions steps. The reason could be that the transition state is preceded by a weak π-complex which is lower in energy than the reactants and transition states (unfortunately a weak π-complex could not be found) or as a result of the basis set superposition error as also found by Haunschild and Frenking for the reactions of $[RhO_2(CH_3)CH_2]$ with ethylene.[45]

4. Conclusion

The following conclusions are drawn from the results presented:

1. On the singlet surface, the [3 + 2] addition leading to the formation of a dioxylate intermediate is the predominantly favored pathway in the complexes studied; it is favored over the [2 + 2] addition pathway leading to the formation of a metallaoxetane intermediate for the complexes $LMnO_3$ (L = O^-, Cp, OCH_3, Cl, CH_3, NPH_3). This is the same as that found by Aniagyei *et al.*[25,26] for the Tc and Re systems with the same set of ligands. The activation barrier and product stabilities for the formation of the dioxylate follow the order $NPH_3 < Cl^- < CH_3O^- < Cp < O^- < CH_3$, which is significantly different from the trend found for the Tc and Re systems in ref. 25 and 26 which is $Cp < Cl^- < CH_3O^- < NPH_3 < CH_3 < O^-$.

2. On the doublet PES, the [3 + 2] addition leading to the formation the dioxylate intermediate is favored over metallaoxetane formation for the ligands L = CH_3. The activation barriers for the formation of the dioxylate intermediate are found to increase for the ligands in the order $CH_3O^- < Cl^- < Cp < CH_3$

while the reaction energies follow the order $Cl^- < CH_3O^- < Cp < CH_3$.

3. Of the group VII B metal oxo complexes studied, MnO_4^- and $MnO_3(OCH_3)$ appear to be the best catalysts for the exclusive formation of the dioxylate intermediate, $MnO_3(OCH_3)$ being better so on both kinetic and thermodynamic grounds. The best epoxidation catalyst for the Mn complexes is MnO_3Cl.

4. The MnO_4^-, $MnO_3(OCH_3)$ and MnO_3Cp reaction surfaces are much 'cleaner' than the rest of the complexes studied, *i.e.* there are no side-reactions competing with the formation of the dioxylate and metallaoxetane intermediates. This trend was also observed for the technetium and rhenium complexes ReO_3L and TcO_3L (L = O^-, Cl, CH_3, OCH_3, Cp, NPH_3); the clean surfaces are found in MnO_4^- and MnO_3Cp.[25,26]

5. The re-arrangement of the metallaoxetane intermediate to the dioxylate is not a feasible reaction for all the ligands studied.

6. There does not appear to be a spin-crossover in any of the pathways studied.

7. The trends observed for the oxidation reactions of the Mn complexes with ethylene compare closely with those reported[25,26] for the ReO_3L and TcO_3L (L = O^-, Cl, CH_3, OCH_3, Cp, NPH_3) complexes, but there is far greater similarity between the Re and Tc complexes than between Mn and either of the other two.

Acknowledgements

The authors are very grateful to the National Council for Tertiary Education (NCTE), Ghana, for a research grant under the Teaching and Learning Innovation Fund (TALIF-KNUSTR/3/008/2005).

References

1 J. H. Enemark and C. G. Young, Bioinorganic Chemistry of Pterin-Containing Molybdenum and Tungsten Enzymes, *Adv. Inorg. Chem.*, 1993, **40**, 1–88.
2 K. B. Sharpless and K. Akashi, Oxidation of alcohols to Aldehydes by reagents derived from chromyl chloride, *J. Am. Chem. Soc.*, 1975, **97**, 5927–5928.
3 W. Mijs and C. R. Jonge, *Organic Synthesis by oxidation with Metal Compound*, Plenum, New York, 1986.
4 M. Sono, M. P. Roach, E. D. Coulter and H. E. Dawson, Heme-Containing Oxygenases, *Chem. Rev.*, 1996, **96**, 2841–2888.
5 K. A. Jorgensen, Transition-metal-catalyzed epoxidation, *Chem. Rev.*, 1989, **89**, 431–458.
6 J. San Filippo and C. Chern, Chemisorbed chromyl chloride as a selective oxidant, *J. Org. Chem.*, 1977, **42**, 2182–2183.
7 M. Schröder, Osmium tetraoxide cis-hydroxylation of unsaturated substrates, *Chem. Rev.*, 1980, **80**, 187–213.
8 K. B. Wiberg, *Oxidation in Organic Chemistry*, Academic Press, New York, 1965, Part A, pp. 1–68.
9 S. Dapprich, G. Ujaque, F. Maseras, A. Lledos, D. G. Musaev and K. Morokuma, Theory Does Not Support an Osmaoxetane Intermediate in the Osmium-Catalyzed Dihydroxylation of Olefins, *J. Am. Chem. Soc.*, 1996, **118**, 11660–11661.
10 U. Pidun, C. Boehme and G. Frenking, Theory Rules Out a [2 + 2] Addition of Osmium Tetraoxide to Olefins as Initial Step of the Dihydroxylation Reaction, *Angew. Chem., Int. Ed. Engl.*, 1996, **35**, 2817–2820.
11 M. Torrent, L. Deng, M. Duran, M. Solä and T. Ziegler, Density Functional Study of the [2 + 2] and [2 + 3] Cycloaddition Mechanisms for the Osmium-Catalyzed Dihydroxylation of Olefins, *Organometallics*, 1997, **16**, 13–19.
12 A. J. Del Monte, J. Haller, K. N. Houk, K. B. Sharpless, D. A. Singleton, T. Strassner and A. A. Thomas, Experimental and Theoretical Kinetic Isotope Effects for Asymmetric Dihydroxylation. Evidence Supporting a Rate-Limiting [3 + 2] Cycloaddition, *J. Am. Chem. Soc.*, 1997, **119**, 9907–9908.
13 D. W. Nelson, A. Gypser, P. T. Ho, H. C. Kolb, T. Kondo, H. Kwong, D. V. McGrath, A. E. Rubin, P. Norrby, K. P. Gable and K. B. Sharpless, Toward an Understanding of the High Enantioselectivity in the Osmium-Catalyzed Asymmetric Dihydroxylation. Electronic Effects in Amine-Accelerated Osmylations, *J. Am. Chem. Soc.*, 1997, **119**, 1840–1858.
14 E. J. Corey and M. C. Noe, Kinetic Investigations Provide Additional Evidence That an Enzyme-like Binding Pocket Is Crucial for High Enantioselectivity in the Bis-Cinchona Alkaloid Catalyzed Asymmetric Dihydroxylation of Olefins, *J. Am. Chem. Soc.*, 1997, **118**, 319–329.
15 J. Haller, T. Strassner and K. N. Houk, Experimental and Theoretical Kinetic Isotope Effects for Asymmetric Dihydroxylation. Evidence Supporting a Rate-Limiting [3 + 2] Cycloaddition, *J. Am. Chem. Soc.*, 1997, **119**, 8031–8034.
16 K. N. Houk and T. Strassner, Establishing the [3 + 2] Mechanism for the Permanganate Oxidation of Alkenes by Theory and Kinetic Isotope Effects, *J. Org. Chem.*, 1999, **64**, 800–802.
17 M. Torrent, L. Deng and T. Ziegler, A Density Functional Study of [2 + 3] versus [2 + 2] Addition of Ethylene to Chromium–Oxygen Bonds in Chromyl Chloride, *Inorg. Chem.*, 1998, **37**, 1307–1314.
18 (*a*) R. Criegee, Osmiumsaure-ester als Zwischenprodukte bei Oxydationen, *Justus Liebigs Ann. Chem.*, 1936, **522**, 75–96; (*b*) R. Criegee, B. Marchaand and H. Wannowius, Zur Kenntnis der organischen Osmium-Verbindungen. II. Mitteilung, *Ann. Chem.*, 1942, **550**, 99–133.
19 K. B. Sharpless, A. Y. Teranishi and J. E. Bäckvall, Chromyl chloride oxidations of olefins. Possible role of organometallic intermediates in the oxidations of olefins by oxo transition metal species, *J. Am. Chem. Soc.*, 1977, **99**, 3120–3128.
20 A. Dauth and J. A. Love, Reactivity by design—Metallaoxetanes as centerpieces in reaction development, *Chem. Rev.*, 2011, **111**, 2010–2047.
21 T. Wistuba and C. Limberg, Reaction of Permanganyl chloride with Olefins: Intermediates and Mechanism as Derived

from Matrix-isolation Studies and Density Functional Theory Calculation, *Chem.–Eur. J.*, 2001, **21**, 4674–4685.
22 T. Strassner and M. Busold, Density Functional Theory Study on the Initial Step of the Permanganate Oxidation of Substituted Alkynes, *J. Phys. Chem. A*, 2004, **108**, 4455–4458.
23 P. Gisdakis and N. Rösch, [2 + 3] Cycloaddition of Ethylene to Transition Metal Oxo Compounds. Analysis of Density Functional Results by Marcus Theory, *J. Am. Chem. Soc.*, 2001, **123**, 697–701.
24 T. Strassner and M. Busold, A Density Functional Theory Study on the Mechanism of the Permanganate Oxidation of Substituted Alkenes, *J. Org. Chem.*, 2001, **66**, 672–676.
25 A. Aniagyei, R. Tia and E. Adei, A density functional theory study of the mechanisms of oxidation of ethylene by rhenium oxide complexes, *Dalton Trans.*, 2013, **42**, 10885–10897.
26 A. Aniagyei, R. Tia and E. Adei, A density functional theory study of the mechanisms of oxidation of ethylene by technetium oxo complexes, *Comp. Theor. Chem.*, 2013, **1009**, 70–80.
27 R. Poli, Open-shell organometallics as a bridge between Werner-type and low-valent organometallic complexes. The effect of the spin state on the stability, reactivity and structure, *Chem. Rev.*, 1996, **96**, 2135–2204.
28 A. Ansari, A. Kaushik and G. Rajaraman, Mechanistic insights on the ortho-hydroxylation of aromatic compounds by non-heme iron complex: A computational case study on the comparative oxidative ability of ferric-hydroperoxo and high-valent Fe^{IV}=O and Fe^{V}=O intermediates, *J. Am. Chem. Soc.*, 2013, **135**, 4235–4249.
29 M. Jaccob and G. Rajaraman, A computational examination on the structure, spin-state energetics and spectroscopic parameters of high-valent Fe^{IV}=NTs species, *Dalton Trans.*, 2012, **41**, 10430–10439.
30 J. N. Harvey, R. Poli and K. M. Smith, Understanding the reactivity of transition metal complexes involving multiple spin states, *Coord. Chem. Rev.*, 2003, **238–239**, 347–361.
31 A. L. Buchachenko, Recent advances in spin chemistry, *Pure Appl. Chem.*, 2000, **72**, 2243–2258.
32 D. Schröder, S. Shaik and H. Schwarz, Two-state reactivity as a new concept in organometallic chemistry, *Acc. Chem. Res.*, 2000, **33**, 139–145.
33 *Spartan*, Wavefunction, Inc., Irvine, CA 92715, USA.
34 T. H. Dunning Jr. and P. J. Hay, in *Modern Theoretical Chemistry*, ed. H. F. Schaefer III, Plenum, New York, 1976, vol. 3.
35 W. R. Wadt and P. J. Hay, Ab initio effective core potentials for molecular calculations. Potentials for the transition metal atoms Sc to Hg, *J. Chem. Phys.*, 1985, **82**, 270–283.
36 W. R. Wadt and P. J. Hay, Ab initio effective core potentials for molecular calculations. Potentials for main group elements Na to Bi, *J. Chem. Phys.*, 1985, **82**, 284–298.
37 W. R. Wadt and P. J. Hay, Ab initio effective core potentials for molecular calculations. Potentials for K to Au including the outermost core orbitals, *J. Chem. Phys.*, 1985, **82**, 299–310.
38 M. Clark, R. D. Cramer and N. V. Opdenbosch, Validation of the general purpose tripos5.2 force field, *J. Comput. Chem.*, 1989, **10**, 982–1012.
39 G. J. Palenik, Crystal structure of potassium manganite, *Inorg. Chem.*, 1967, **6**, 507–511.
40 R. Tia and E. Adei, [3 + 2] versus [2 + 2] addition of metal oxides across C=C bonds: A theoretical study of the mechanism of oxidation of ethylene by osmium oxide complexes, *Comp. Theor. Chem.*, 2011, **977**, 140–147.
41 U. Pidun, C. Boehme and G. Frenking, Theory Rules Out a [2 + 2] Addition of osmium tetraoxide to olefins as initial step of the dihydroxylation reaction, *Angew. Chem., Int. Ed. Engl.*, 1996, **35**, 2817–2820.
42 M. Torrent, L. Deng, M. Duran, M. Sola and T. Ziegler, Mechanism for the formation of epoxide and chlorine-containing products in the oxidation of ethylene by chromyl chloride: a density functional study, *Can. J. Chem.*, 1999, **77**, 1476–1491.
43 S. Dapprich, G. Ujaque, F. Maseras, A. Lledos, D. G. Musaev and K. Morokuma, Theory does not support an osmaoxetane intermediate in the osmium-catalyzed dihydroxylation of olefins, *J. Am. Chem. Soc.*, 1996, **118**, 11660–11661.
44 R. Tia and E. Adei, Density functional theory study of the mechanism of oxidation of ethylene by chromyl chloride, *Inorg. Chem.*, 2009, **48**, 11434–11443.
45 R. Haunschild and G. Frenking, Theoretical studies of organometallic compounds. 60. Ethylene addition to group-9 transition metal dioxo compounds - A quantum chemical study, *Z. Anorg. Allg. Chem.*, 2008, **634**, 2145–2155.